Exploiting the Phantom-Mode Signal in DSL Applications

Wim Foubert, Carine Neus, Leo Van Biesen, and Yves Rolain

***Abstract*—In order to meet the ever-increasing bandwidth demand of the users, new "digital subscriber line" (DSL) technologies are being developed. In addition to the traditional differential mode of the telephone line, telecom operators are now looking in to the exploitation of the phantom-mode signal. New transmission line models, using the multiconductor transmission lines theory, were developed to support this extended use. In this paper, it is shown that the phantom mode is an eigenmode of the quad cable system, and hence, according to the theory, there is no crosstalk between this mode and the differential mode.**

***Index Terms*—Digital subscriber line (DSL) technologies, multiconductor transmission line, phantom mode, quad.**

I. Introduction

A. DSL Technology

DIGITAL subscriber line (DSL) technology enables high-speed digital transmission over the copper-twisted pairs of the existing telephone network [1]. The twisted-wire-pair infrastructure was originally designed to provide a reliable plain old telephone service only [2]. This means that the lines were constructed to carry a single voice signal with frequencies varying from 300 Hz up to 3.4 kHz (voiceband). All DSL technologies make use of much higher frequencies, of course, at the cost of a reduced range.

B. State of the Art

The increasing users' demand for high-bandwidth applications encourages the development and the deployment of new broadband access technologies. The overview of the deployment volumes (the number of new installations or upgrades) of the successive access techniques over time given by Ödling *et al.* [3] clearly shows that, because of the high costs involved in deploying fiber, optical fibers will only enter customer premises very gradually in the coming years. As a consequence, copper has still an important role to play. Nowadays, one is looking into new methods to further increase the bitrate on copper. In general, there are three different possible ways to achieve this goal. All the state-of-the-art DSL technologies use one of those methods.

A first alternative extends the concept of a two-wired line. It uses vector signals to transmit a single circuit. An increased throughput is obtained by coordinating the transmission at the source side and the reception at the receiver side. The binder that connects the central office and the last distribution point contains hundreds of twisted pairs. The vectored source can reduce and/or exploit crosstalk, particularly near-end crosstalk (NEXT) [4], to increase cable-level throughput. This results in vectoring, where only the transmitters are colocated.

In multiple-input–multiple-output (MIMO) DSL, both the transmitters and the receivers are vectored or colocated. This buys additional degrees of freedom and enables to ideally eliminate both the far-end crosstalk (FEXT) and the NEXT. The MIMO channel response function has already been modeled by Jakovljevic *et al.* [5] and Lee *et al.* [6] and increases the cable-level throughput further.

Another way to increase the bitrate is by breaking the conventional pairs into two wires to get more circuits when each wire is used with respect to ground to convey a signal. This is possible as some DSL binders consist of one or more layers of metallic sheath enclosing the wire pairs. The grounded shield can then be treated as a third conductor. It will be used as the return path for the common-mode signal [7], [8].

Instead of using the shield, one wire in one of the pairs can also be taken as a reference wire. This idea relies on a lumped model for the cable, as unbundling results in a very different characteristic impedance for the different transmission lines. In [9], Cioffi *et al.* studied this use of "split pairs," also called "single-wire excitation." For the cable of the last mile entering the user premises, a quad (two-pair cable) is often used. In a quad, there are three circuits in a split-pair setup (between the three remaining wires of the quad and the reference) instead of two. However, in a real installed network, each pair is loaded by a balun which hampers the implementation of this split.

In the rest of this paper, we will focus on a third possible alternative that will be applied on the last segment of the access network. The idea is to combine the advantages of the previous approaches ("vectoring" and "breaking the circuit") to maximize the practical usability of the method without the need for rewiring. It results in an approach that is dual to the unbundling in the sense that it relies on a distributed model of the cable. To this end, we will continue to use differential signaling only, to avoid the pitfalls of an uncertain return path. We will use the eigenmodes of the cable system as orthogonal-independent circuits instead, since we know that, theoretically speaking,

Manuscript received April 12, 2011; revised July 19, 2011; accepted October 5, 2011. Date of publication December 19, 2011; date of current version March 9, 2012. This work was supported in part by the Fund for Scientific Research (FWO Vlaanderen), by the Flemish Government (Methusalem Fund METH1), and by the Belgian Government (IUAP VI/4, DYSCO). The Associate Editor coordinating the review process for this paper was Dr. Matteo Pastorino.

The authors are with the Department of Fundamental Electricity and Instrumentation, Vrije Universiteit Brussel, 1050 Brussels, Belgium (e-mail: wfoubert@vub.ac.be).

Color versions of one or more of the figures in this paper are available online at http://ieeexplore.ieee.org.

Digital Object Identifier 10.1109/TIM.2011.2174100

0018-9456/$26.00 © 2011 IEEE

those modes do not influence each other. Consequently, if it should be possible to exploit all the eigenmodes, the achievable bitrate should increase. We will see that, in this way, three independent differential signaling paths can also be obtained for a quad cable.

C. Phantom-Mode Signals

As the access network from the last departure point to the home often contains two pairs that are wired as a quad, this topology is a very important one. The current state-of-the-art DSL systems use only one differential-mode signal that travels on one single telephone pair. In the near future, it is expected that the four wires will be exploited together.

In this paper, three differential and mutually orthogonal signal paths are shown to be present in this configuration. The port condition is respected, and a full differential setup that matches the one used in the current infrastructure is used. In addition to the standard differential-mode signal on each pair, an extra "phantom mode" pairwise differential signal in between the pairs is used [10]. This signal is transported independently of the two other pair signals as it corresponds to the voltage difference between the arithmetic mean of the voltages on the two conductors of each pair. In this way, the "phantom-mode" signal is also a differential-mode signal, but it uses all four wires simultaneously to carry the signal. It is, therefore, pretty much a cable-based implementation of the vectoring approach. As already mentioned earlier, this paper looks for the propagation eigenmodes of the quad since they are, theoretically speaking, immune to crosstalk. In order to determine these eigenmodes, we need an accurate physical quad model.

In Section II, the quad cable model is derived based on the multiconductor transmission line theory. In Section III, the eigenmodes of the four-wire system are determined. In Section IV, we will investigate if our orthogonality assumption holds: The cable will be excited in one mode, and it will be investigated how the other modes are influenced. Finally, the most important conclusions are summarized in Section V.

II. Modeling a Quad Cable

A. Multiconductor Transmission Line Theory

To model a multiconductor cable, several possibilities exist. The most straightforward way is to derive a model based on measurements [11]. However, in this paper, a quad line will be modeled using the multiconductor transmission line theory [12]. The multiconductor transmission line theory relies on the basic assumption of a uniform line of infinite length. Consider now an infinitesimal longitudinal section of such a line. Fig. 1 shows the schematic diagram that models a single pair of the homogeneous line. This can easily be expanded to the four-wire case, but the graphical representation becomes complex as R, L, G, and C become 4×4 real per-unit matrices called, respectively, the resistance matrix R, the inductance matrix L, the conductance matrix G, and the capacitance matrix C. A good characterization of these matrices is indispensable to obtain reliable physical models of the cable behavior.

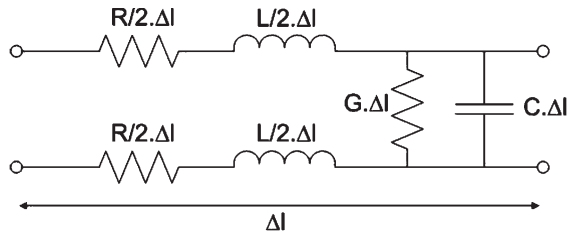

Fig. 1. Infinitesimal section of length Δl of a two-wire transmission line; extension to a quad is straightforward but crowded.

B. Determination of the Per-Unit Matrices

These matrices are obtained for the given geometry. The full electromagnetic problem is decoupled into a transversal and a longitudinal subproblem. Since the diameter of the quad is much smaller than the wavelength of the transported signals, a quasi-static field approximation can safely be used in the transversal plane. This allows one to determine the impedance matrix and the admittance matrix, yielding the characteristic impedance and the propagation constant. The resistance matrix R and the inductance matrix L of the model are determined via a Newtonian potential formulation [10]. The series impedance model has been validated in previous work with reflection measurements [13]. A numerical approximation technique is used to characterize the capacitance matrix C. The last parameter that we must determine in the transversal plane is the conductance matrix G. This only depends on the properties of the dielectric. In practice, polyethylene is used as an isolator. Fortunately, the relative permittivity of polyethylene can be assumed to be independent of the frequency in the considered frequency band (0.1–25 MHz), and almost no dielectric losses occur. As a consequence, G can safely be assumed to be a constant matrix over the usable frequency band.

C. Relation Between Input and Output Voltages and Currents

Once the $RLGC$ per-unit matrices of the quad cable have been calculated, we are able to model the behavior of the line using the transmission line equations given hereinafter as a function of the frequency in harmonic regime [12]

$$\begin{cases} -\frac{dV}{dz} = (R + j\omega L)I = ZI \\ -\frac{dI}{dz} = (G + j\omega C)V = YV \end{cases} \tag{1}$$

where $Z = R + j\omega L$ is the impedance matrix per unit length $\in \mathbb{C}^{4\times4}$ and $Y = G + j\omega C$ is the admittance matrix per unit length $\in \mathbb{C}^{4\times4}$. I and V are, respectively, the current and the voltage vector $\in \mathbb{C}^{4\times1}$ at $z = z_0$. Combining both equations in (1), we find a second-order differential system of equations, with respect to the longitudinal coordinate z

$$\frac{d^2I(z)}{dz^2} = YZI(z). \tag{2}$$

This equation is an eigenequation. The eigenvalues of the matrix YZ are to be determined. In general, as long as YZ is of full rank, it is always possible to find a nonsingular transformation matrix T, which diagonalizes the product of the per-unit length admittance and impedance matrices YZ [12]

$$T^{-1}YZT = \gamma^2. \tag{3}$$

Here, γ^2 is a diagonal $\mathbb{C}^{4\times4}$ matrix with scalar complex values γ_i^2 on the diagonal. These γ_i^2 are the eigenvalues of the matrix YZ. The columns of the orthonormal matrix T are the eigenvectors of the matrix.

Consider now a line segment of finite length L. The voltages and the currents at the two ends of the line can be related by the chain parameter matrix $\phi(L)$ [12]

$$\begin{bmatrix} V(L) \\ I(L) \end{bmatrix} = \begin{bmatrix} \phi_{11}(L) & \phi_{12}(L) \\ \phi_{21}(L) & \phi_{22}(L) \end{bmatrix} \begin{bmatrix} V(0) \\ I(0) \end{bmatrix}. \tag{4}$$

The submatrices are obtained by the following relations that depend on the eigendecomposition [12]:

$$\begin{cases} \phi_{11} = \frac{1}{2}Y^{-1}T(e^{\gamma l} + e^{-\gamma l})T^{-1}Y \\ \phi_{12} = -\frac{1}{2}Y^{-1}T\gamma(e^{\gamma l} - e^{-\gamma l})T^{-1} \\ \phi_{21} = -\frac{1}{2}T(e^{\gamma l} - e^{-\gamma l})\gamma^{-1}T^{-1}Y \\ \phi_{22} = \frac{1}{2}T(e^{\gamma l} + e^{-\gamma l})T^{-1}. \end{cases} \tag{5}$$

With those equations, one is able to calculate the port current flowing in and the voltage difference across each port at both ends of the line. One can also turn the problem inside out and determine the pattern of currents and voltages that define an eigenmode of the transmission line.

III. Eigenmodes

According to the multiconductor transmission line theory, for each type of cable, specific propagation eigenmodes exist [12]. These correspond to specific distributions of voltages and currents that propagate with their own phase velocity and lineic attenuation but are independent from each other. Now, the properties of the eigenmodes of the quad cable will be investigated. Therefore, the eigenvalues and the corresponding eigenvectors of the quad are calculated using (3). The considered quad consists of four conductors that are placed in a square formation where each conductor has the same radius (0.425 mm) and the distance between the centers of two neighboring conductors is 4.2 mm. There is no ground connection between both ends of the line in this setup. The square root γ_i of the eigenvalues γ_i^2 is plotted in Fig. 2 as a function of the frequency. γ_i represents the propagation constant of the ith eigenmode of the line. It can be split in a real and an imaginary part

$$\gamma_i(f) = \alpha_i(f) + j\beta_i(f). \tag{6}$$

The real part $\alpha_i(f)$ represents the frequency-dependent attenuation constant. Hence, it models the attenuation of a quasi-TEM wave propagating through the medium. The imaginary part $\beta_i(f)$ is called the phase constant and determines the phase velocity of the considered eigenwave. Both the real and the imaginary parts are shown in Fig. 2 for all the eigenvalues. We see that the first propagation constant γ_1 is zero and corresponds to a mode that does not propagate over the line. The third (γ_3) and fourth (γ_4) eigenvalues are exactly equal. This implies that a double eigenvalue is present and results in an eigenplane rather than an eigenvector, which is associated to the double eigenvalue. The second propagation factor γ_2 has the same phase constant as γ_3 and γ_4, but its attenuation constant is different.

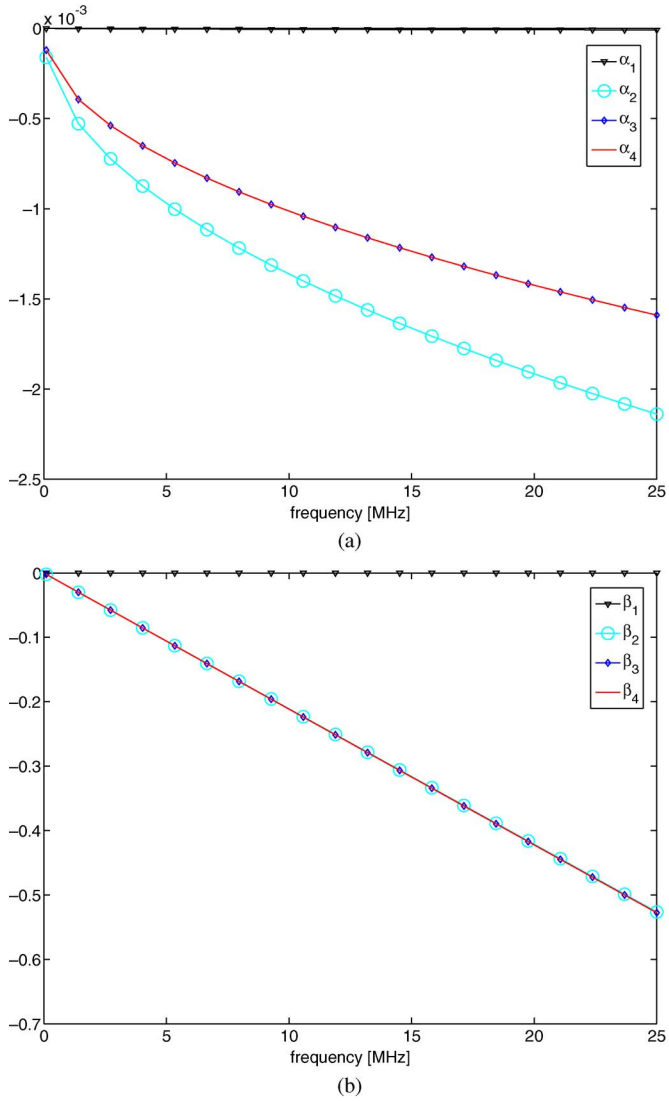

Fig. 2. (a) Real and (b) imaginary parts of the propagation constant of the eigenmodes versus frequency.

First, we take a look at the eigenvectors associated to the eigenvalues and their evolution as a function of the frequency. In this way, we learn more about the structure of the eigenmodes. This will enable us to get insight in the differences and the similarities between the modes and their relation to the eigenvalues. Each eigenvector consists of four complex numbers that are shown in Figs. 3–5. The x-coordinate gives the real part, whereas the y-coordinate corresponds to the imaginary part of the number. The numbers represent the direction and the magnitude of the currents in the four conductors of the quad. The direction of the currents for the different modes is shown in Fig. 6. A cross indicates that the current flows into the cross section. A bullet denotes that the current flows out the cross section.

The eigenvector belonging to the first eigenvalue consists of four times the same current value (see Fig. 3). As a consequence, the currents in the four wires are equal in magnitude and flow in the same direction. There is no return path other than the conductor at ∞ as can be seen in Fig. 6. This explains why the first propagation constant is zero: This mode

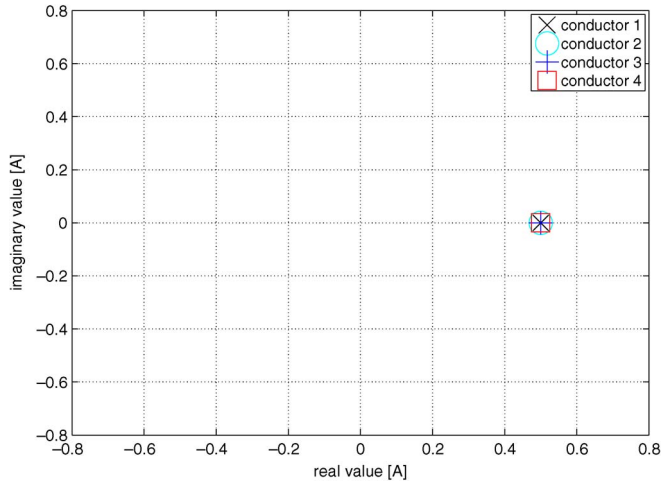

Fig. 3. Eigenmode 1.

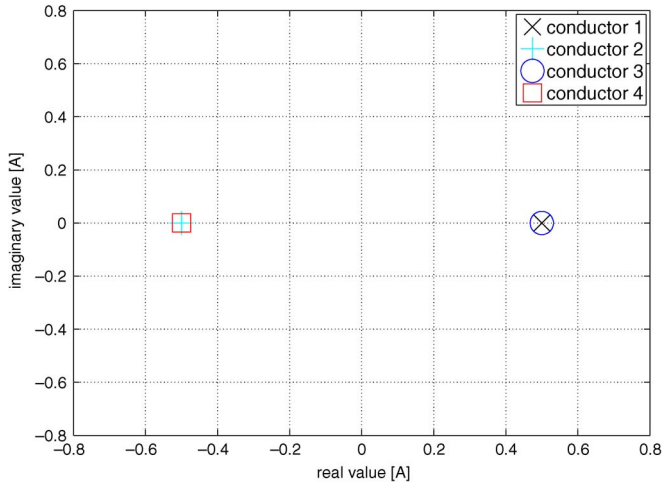

Fig. 4. Eigenmode 2.

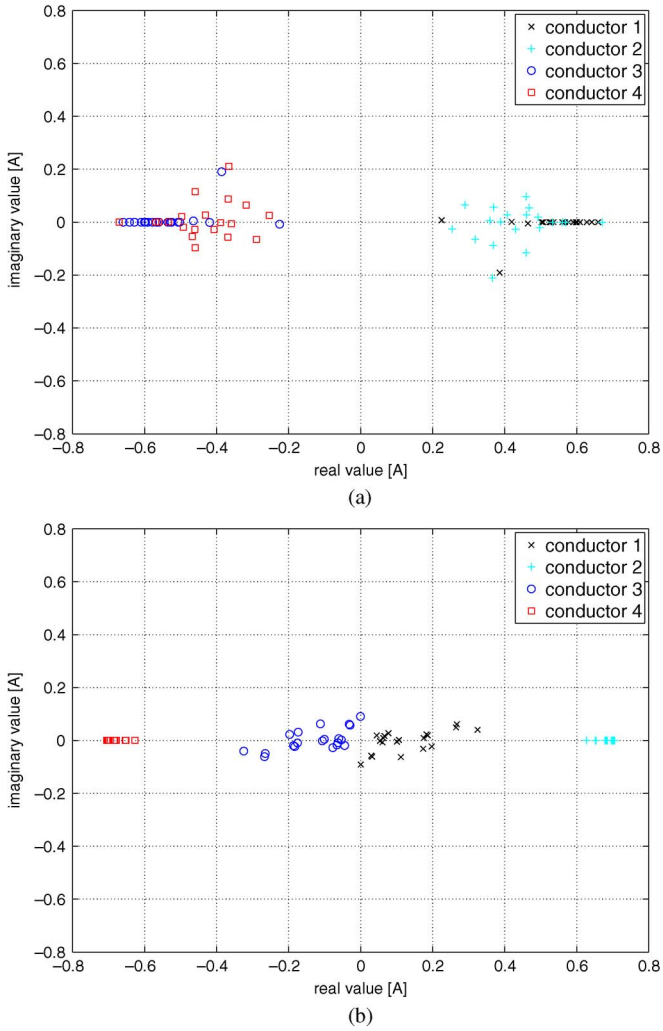

Fig. 5. (a) Eigenmode 3. (b) Eigenmode 4.

is physically unrealizable without the presence of the reference conductor at ∞.

Consider now the second eigenvector (Fig. 4). The magnitude of the currents in all the conductors is again the same. However, now, the current in the second and the fourth wire flows in the opposite sense as the current in the first and the third conductor. One can think of the second and the fourth conductor as the return path for the current. The port condition on the current is therefore met by this mode, and propagation occurs. This mode corresponds to the phantom mode of propagation (see Fig. 6). This means that the phantom mode is indeed an eigenmode of the system.

The eigenvectors belonging to the third and the fourth eigenvalue are similar but look a lot more messy over the frequency (Fig. 5). In both cases, two pairs of currents can be distinguished. The first and third elements of the eigenvector have an opposite sign and equal magnitude. Consequently, the first and third wires present a separate forward and return path for a current and act as a separate circuit. They account for the first pair. The second and fourth elements of both eigenvectors also have opposite sign and equal magnitude, but the magnitudes of the two pairs are different. Conductors 2 and 4 constitute the second pair. The amplitude of the currents in the two pairs is different. The corresponding figures for the last two cases in Fig. 6 show only the direction of the currents. As mentioned before, the amplitude of the current is the same in the wires constituting a pair but is different from pair to pair. The last two eigenmodes, therefore, also require a current to flow in the four wires, and hence, the pairwise propagation that is commonly used seems not to be an eigenmode of the cable.

One has to be careful, however, that, as the eigenvalues associated with the last two modes are exactly equal, this eigenvalue has a multiplicity of two. Since the eigenvectors are linearly independent by construction, one must take the following theorem into consideration:

Theorem 1: If $\vec{x}, \vec{y}, \vec{z}, \ldots$ are linearly independent eigenvectors of an operator A corresponding to the same eigenvalue and $\alpha, \beta, \zeta, \ldots$ are arbitrary numbers belonging to the same field as the elements of the matrix A, then the vector $\alpha\vec{x} + \beta\vec{y} + \zeta\vec{z} + \ldots$ is also an eigenvector corresponding to the same eigenvalue.

For the proof, see [14]. In other words, the linearly independent eigenvectors (also called characteristic vectors) form a basis of a "characteristic" subspace. Each vector in this subspace is again an eigenvector associated to the same eigenvalue. As a consequence, each linear combination of the third and the fourth eigenvector is also an eigenvector of the last eigenvalue.

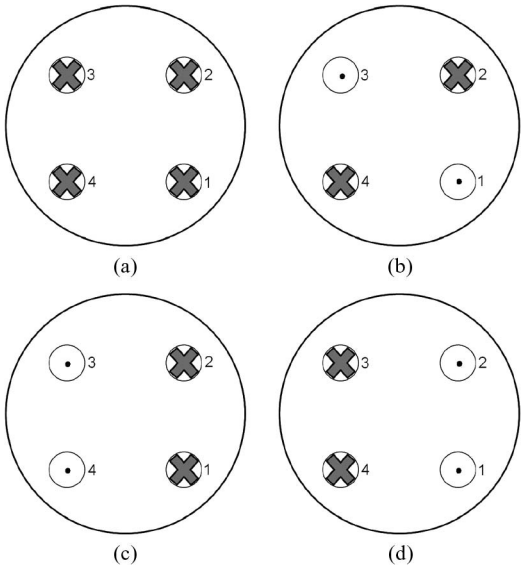

Fig. 6. Current distribution for the different eigenmodes. (a) Eigenmode 1. (b) Eigenmode 2. (c) Eigenmode 3. (d) Eigenmode 4.

It can be shown that the two differential pair modes form a basis of the characteristic subspace too, by applying a well-chosen linear combination

$$\begin{cases} DM1 = T(:,3) - \frac{T(1,3)}{T(1,4)}T(:,4) \\ DM2 = T(:,3) - \frac{T(2,3)}{T(2,4)}T(:,4). \end{cases} \quad (7)$$

In those equations, $T(:,3)$ and $T(:,4)$ are, respectively, the third and the fourth column of matrix T that diagonalizes the original matrix [as found in (3)], and they represent the third and the fourth eigenvector. $T(1,3)$ and $T(2,3)$ are the first and the second value of the third eigenvector. Similarly, $T(1,4)$ and $T(2,4)$ are the first and the second element of the fourth eigenvector. In the first differential mode $(DM1)$, neither the first nor the third wire carries current. Only conductors 2 and 4 are used. In the second differential mode $(DM2)$, the current flows in the other pair. This means that, in addition to the phantom mode, also the two differential modes are shown to be eigenmodes of the system.

As the differential mode uses only two conductors, whereas the phantom mode exploits the four wires, a difference in attenuation constant between the differential and phantom modes is to be expected. In phantom mode, the wave attenuation coefficient is approximately 30% higher than in differential mode as can be noticed from the attenuation function in Fig. 2. The phase function shows that the velocity of the waves is the same in phantom mode as in both differential modes. This is an important point, as this means that no difference in propagation delay will exist between the eigenmodes.

IV. Crosstalk

In this section, the main goal is to determine whether the theoretically expected absence of crosstalk between the different modes is indeed supported by simulations. To verify this, the system will be carefully excited in one mode at the input, and the currents in the conductors at the output will be investigated.

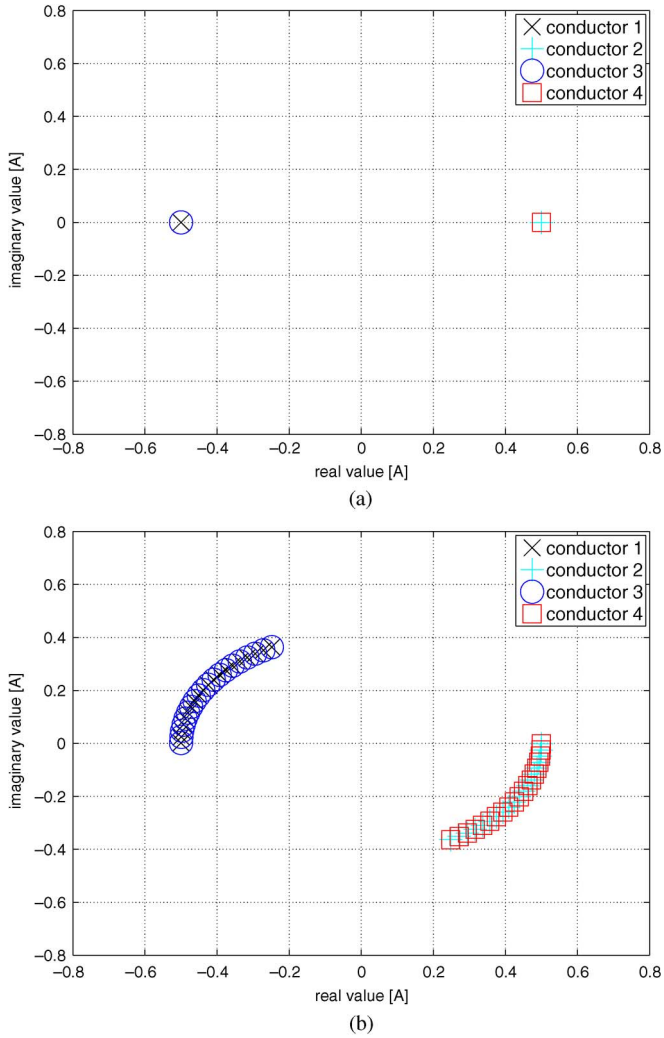

Fig. 7. Currents at the (a) near and (b) far ends of the cable for each wire when the quad is excited in phantom mode. (a) Input. (b) Output.

In the first experiment, the quad is excited in phantom mode. The amplitude of the currents is the same in the four wires, but the currents in conductors 2 and 4 flow in the opposite sense as the currents in wires one and three. Those currents are plotted in the first picture (a) in Fig. 7. Simulations are repeated for 20 frequencies spread over a band from 100 kHz to 25 MHz.

Next, the currents at the end of each line are calculated frequency by frequency using the chain parameter matrix (4). In the second plot (b) in Fig. 7, the currents at the end of the line are shown.

They are exactly equal for the first and the third conductor and have opposite sign for the second and the fourth one. At the far end, the four wires still carry a current of equal amplitude, but the current flows in the opposite sense in wires 2,4 and 1,3. Again, we obtain a pure phantom mode. Hence, if we excite the system in phantom mode, then the response of the line consists of a phantom mode alone as expected.

In the next experiment, the quad will be used in differential mode. We will investigate if this will induce a crosstalk signal on the nonexcited lines. When the first differential mode (only current in wire two and wire four) is excited at the near-end input (see Fig. 8), there is indeed no current flowing at the

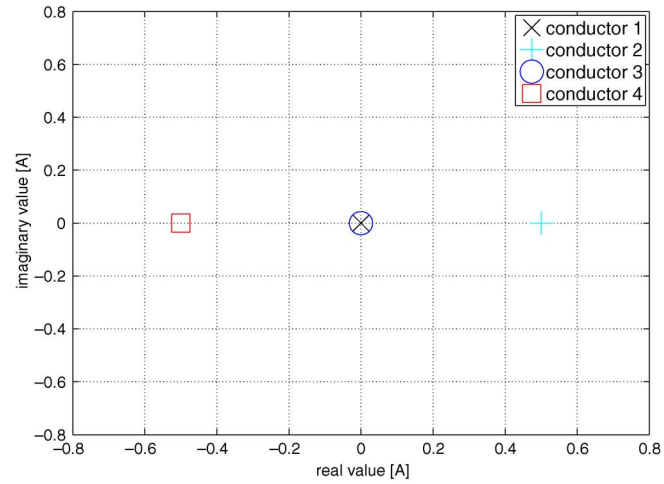

(a)

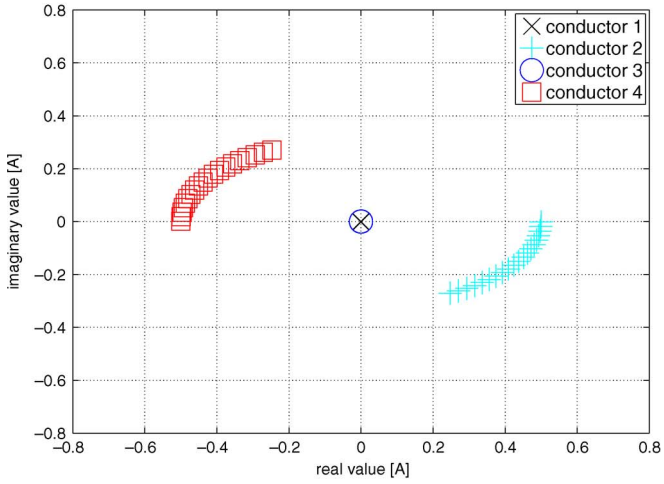

(b)

Fig. 8. Currents at the (a) near and far (b) ends of the cable for each wire when the quad is excited in differential mode. (a) Input. (b) Output.

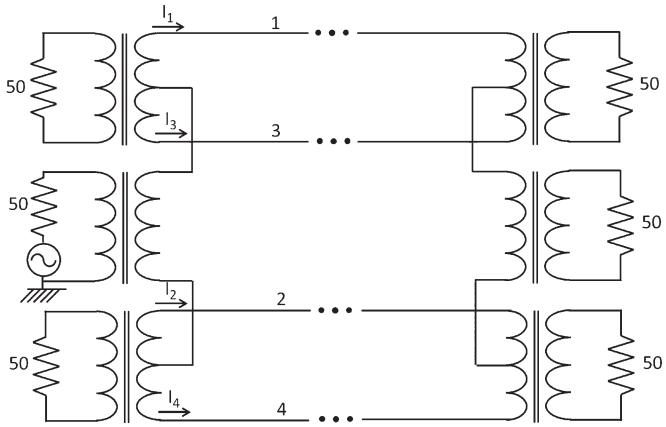

Fig. 9. Setup used to measure the transfer function and the crosstalk when the quad line is operating in phantom mode.

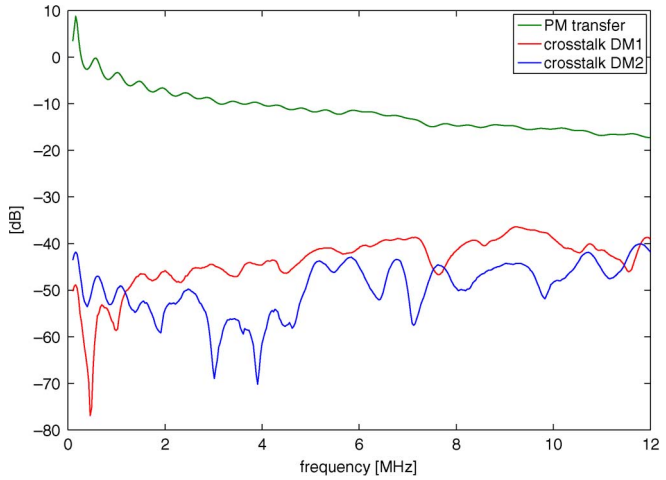

Fig. 10. Transfer function and crosstalk functions when the quad is operating in phantom mode.

far-end output of the second pair that consists of wire one and wire three. Neither the second differential mode nor the phantom mode is influenced by the excitation. The same result holds when the other differential mode (using wire one and wire three) is applied on the quad. Hence, if the system is excited in a strict single-mode setting, only the same mode is found at the output. No crosstalk appears on the other modes. This means that exploitation of the phantom mode will indeed lead to higher bandwidth capacity, since an extra signal path is defined that is independent of the classical differential-mode signal paths.

V. Experimental Verification

Now, the previous results will be verified with measurements on a twisted Belgacom quad line that has a length of 200 m. The radius of each conductor is 0.25 mm, and the distance between the centers of two neighboring conductors is 0.9 mm. The schematic of the measurement setup, used to excite the system in phantom mode, is shown in Fig. 9.

Both at the near end and at the far end of the line, three baluns are used to guarantee the port operation. The upper baluns connect conductors 1 and 3. The lower baluns make the connection between conductors 2 and 4. The center taps of the outer baluns are connected via a center balun. All baluns are terminated in a 50-Ω resistance, except the center balun at the input side of the line where a 50-Ω source is used such that the quad is operating in phantom mode.

The measurements are executed at the external side of the baluns. In this way, the baluns are taken as an integral part of the transmission line. Since an isolation transformer is always present on a line card in the DSLAM, this is representative for the real-world situation. To determine the phantom-mode transfer function, the voltage is measured at the external side of the center balun at the far end. For the determination of the crosstalk between the phantom mode and the two single-pair differential modes, the voltage at the two outer baluns is measured. The transfer function and the FEXT functions are shown in Fig. 10. Care should be taken because those measurements are not calibrated yet. However, this is not so important since one is only interested in the difference in magnitude between the transfer function and the crosstalk and not really in the magnitude of each function individually. The difference should be as big as possible since this will determine the available capacity.

As expected, the transfer function is decreasing with increasing frequency. Because the measurements are not calibrated, the transfer function is larger than 0 dB at low frequencies. The difference in magnitude between the transfer function and the crosstalk functions is decreasing from 45 dB at 1 MHz to 23 dB at 12 MHz. This proves that the crosstalk is small but not really negligible.

Similar experiments were executed for a quad operating in a single-pair differential mode. The same conclusion can be derived.

VI. Conclusion

In new DSL technologies, the phantom-mode signal, defined between two pairs, will also be exploited in addition to the conventional differential-mode signal on one pair. In this way, three signal paths can be defined for a quad. In this paper, it has been shown that both the two differential-mode signals and the phantom-mode signal are eigenmodes of the system. Simulations also show that those three modes do not influence each other. The measurements confirm that the crosstalk is indeed very small between the different modes. However, it is not negligible. Since the crosstalk is very small, this new technology will strongly increase the achievable capacity and consequently support higher bandwidth applications. This increase will be even much stronger when combining this technique with vectoring.

References

[1] T. Star, J. Cioffi, and P. Silverman, *Understanding Digital Subscriber Line Technology*. Upper Saddle River, NJ: Prentice-Hall, 1999.

[2] T. Star, M. Sorbara, J. Cioffi, and P. Silverman, *DSL Advances*. Upper Saddle River, NJ: Prentice-Hall, 2003.

[3] P. Ödling, M. Magesacher, S. Höst, P. Börjesson, M. Berg, and E. Areizaga, "The fourth generation broadband concept," *IEEE Commun. Mag.*, vol. 47, no. 1, pp. 62–69, Jan. 2009.

[4] G. Ginis and M. Cioffi, "Vectored transmission for digital subscriber line systems," *IEEE J. Sel. Areas Commun.*, vol. 20, no. 5, pp. 1085–1104, Jun. 2002.

[5] M. Jakovljevic, T. Magesacher, P. Ödling, P. O. Börjesson, M. Sanchez, and S. Zazo, "Throughput of shielded twisted-pair cables using wire-shield modes in the presence of radio ingress," in *Proc. 16th Int. Conf. Digital Signal Process.*, 2009, vol. 1/2, pp. 1289–1294.

[6] B. Lee, J. M. Cioffi, S. Jagannathan, K. Seong, Y. Kim, M. Mohseni, and M. H. Brady, "Binder MIMO channels," *IEEE Trans. Commun.*, vol. 55, no. 8, pp. 1617–1628, Aug. 2007.

[7] M. Jakovljevic, T. Magesacher, K. Ericson, P. Ödling, P. O. Börjesson, and S. Zazo, "Common mode characterization and channel model verification for shielded twisted pair (STP) cable," in *Proc. IEEE Int. Conf. Commun.*, 2008, vol. 1–13, pp. 447–451.

[8] T. Magesacher, P. Ödling, P. O. Börjesson, and T. Nordström, "Exploiting the common-mode signal in xDSL," in *Proc. EUSIPCO*, Vienna, Austria, Sep. 2004, pp. 1217–1220.

[9] J. M. Cioffi, S. Jagannathan, M. Mohseni, and G. Ginis, "CuPON: The copper alternative to PON 100 Gb/s DSL networks," *IEEE Commun. Mag.*, vol. 45, no. 6, pp. 132–139, Jun. 2007.

[10] V. Belevitch, "Theory of the proximity effect in multiwire cables," *Philips Res. Rep.*, vol. 32, pp. 16–43, 1977.

[11] T. Magesacher, P. Ödling, P. O. Börjesson, and T. Nordström, "Verification of multipair copper-cable model by measurements," *IEEE Trans. Instrum. Meas.*, vol. 56, no. 5, pp. 1883–1886, Oct. 2007.

[12] C. R. Paul, *Analysis of Multiconductor Transmission Lines*. Hoboken, NJ: Wiley, 1994.

[13] W. Foubert, P. Boets, L. Van Biesen, and C. Neus, "Modeling the series impedance of a quad cable for common mode DSL applications," *IEEE Trans. Instrum. Meas.*, vol. 59, no. 2, pp. 259–265, Feb. 2010.

[14] F. Gantmachter, *The Theory of Matrices*, vol. 1. New York: Chelsea, 1959.

Wim Foubert was born in Geraardsbergen, Belgium, on February 14, 1983. He received the B.S. degree in electrical engineering (option electronics and information processing) from Vrije Universiteit Brussel, Brussels, Belgium, in July 2006, where he has been currently working toward the Ph.D. degree in the Department of Fundamental Electricity and Instrumentation since December 2006.

His main research interests are on the design of new transmission channel models for digital subscriber line technology systems.

Carine Neus was born in Anderlecht, Belgium, on March 16, 1983. She received the B.S. degree in electrical engineering and the Ph.D. degree from Vrije Universiteit Brussel, Brussels, Belgium, in 2004 and 2011, respectively.

She is currently a Postdoctoral Researcher with the Department of Fundamental Electricity and Instrumentation, Vrije Universiteit Brussel. Her main interests are in the field of telecommunications, primarily digital subscriber line technologies (xDSL). Her current work is on the modeling of the channel transfer function and the crosstalk of xDSL lines, and the assessment on the achievable data rates.

Leo Van Biesen was born in Elsene, Belgium, on August 31, 1955. He received the B.S. degree in electromechanical engineering and the Ph.D. degree from Vrije Universiteit Brussel, Brussels, in 1978 and 1983, respectively.

He is a Full Senior Professor with Vrije Universiteit Brussel. He teaches courses on fundamental electricity, electrical measurement techniques, signal theory, computer-controlled measurement systems, telecommunication, underwater acoustics, and geographical information systems for sustainable development of environments. His current interests are signal theory, modern spectral estimators, time-domain reflectometry, wireless local loops, digital subscriber line technologies, underwater acoustics, and expert systems for intelligent instrumentation.

Dr. Van Biesen was the President of the International Measurement Confederation (IMEKO) until September 2006. He is also a member of the board of the European Telecommunication Engineers Federation (FITCE) Belgium and the International Scientific Radio Union (URSI) Belgium. He was the Chairman of IMEKO TC-7 from 1994 to 2000, a President Elect of IMEKO for the period 2000–2003, and a Liaison Officer between the IEEE and IMEKO.

Yves Rolain is currently active with the Department of Fundamental Electricity and Instrumentation, Vrije Universiteit Brussel, Brussels, Belgium. His main research interests are nonlinear microwave measurement techniques, applied digital signal processing, parameter estimation/system identification, and biological agriculture.